

## ILLUMINATION AND IMAGE PROCESSING FOR REAL-TIME CONTROL OF DIRECTED ENERGY DEPOSITION ADDITIVE MANUFACTURING

D. Seltzer\*, J. L. Schiano\*, A. R. Nassar†, and E. W. Reutzel†

\*School of Electrical Engineering and Computer Science,  
The Pennsylvania State University, University Park, PA 16802

†Applied Research Laboratory at The Pennsylvania State University, University Park, PA 16802

### Abstract

This paper describes the optical setup and image processing required to estimate melt-pool width and build height for real-time control of melt-pool geometry in directed energy deposition additive manufacturing. To overcome optical interference from plasma emissions and laser interactions, the melt-zone is imaged using laser illumination. A single camera, fixed to the processing laser, views the laser interaction zone and provides images for estimating melt-zone width and build height. Using a bandpass filter and a single aspheric lens, the camera system provides sufficient magnification and depth of field to achieve a 1-mil (25.4  $\mu\text{m}$ ) resolution. Maintaining melt-zone geometry within desired tolerances requires an image acquisition and processing rate on the order of 100 frames per second. This bandwidth is achieved by a Camera Link camera and field-programmable gate array that implements algorithms for estimating melt-pool width and build height. The design and experimental verification of the camera, illumination, and processing systems are discussed.

### 1. Introduction

In order to provide vision-based feedback control, which is essential for maintaining part quality in metal-based additive manufacturing (AM) processes, images of melt-pool geometry must be both acquired and processed in real-time. Based on previous studies [1], in order to obtain images without interference from black body and plasma-plume emissions caused by laser interaction it is necessary to illuminate and image the melt-pool. For this work we used light at a 405 nm wavelength in order to take advantage of the lower plasma-plume emission intensity at the given wavelength. Melt-pool geometry measurements obtained in real-time from this vision system are then verified using post-deposition measurements with an optical profilometer.

The aim of this work is to design an imaging system that can determine build height and melt-pool width for later use in a vision-based feedback control system. The intended final goal being a real-time feedback control system that regulates build height and melt-pool width by controlling scanning speed and laser power inputs to the system.

Two results can be concluded from this work. First, 405 nm is a viable wavelength for illuminating and imaging the melt-pool during the AM process. Second, it is necessary that the imaging system has both sufficient illumination and speed for obtaining real-time measurements.

## 2. Experimental Setup

The AM processing experiments used an Optomec LENS MR-7 directed-energy-deposition system. The LENS system utilizes a 500 W, Ytterbium-doped fiber-laser (IPG YLR-500-SM). The working distance is 0.365 in, measured from the substrate to four radially-symmetric power delivery nozzles. Centered within the nozzles is a center-purge nozzle through which argon flows coaxially onto the substrate.

A custom mounting fixture, shown in Figure 1, extends from the laser processing head. Mounted on this fixture is a monochrome camera and a 405 nm illumination source, both aimed at the front of the melt-pool such that the melt-pool appears to be moving towards the camera. The optical axis of the camera is approximately  $15^\circ$  with respect to the substrate. An additional custom mounting fixture surrounds the laser processing head. Mounted on this fixture are four radially-symmetric 405nm illumination sources.

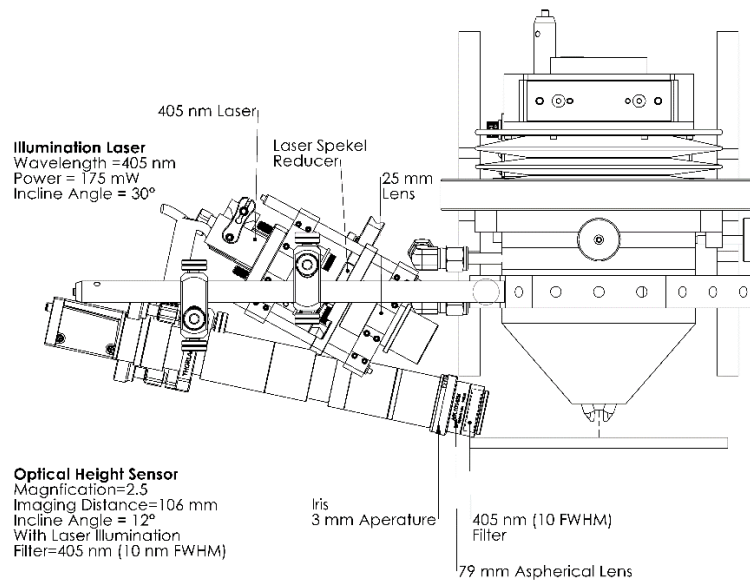


Figure 1. Camera and initial illumination system mounting fixture.

The camera used is an ACER model acA2040-180km Camera Link camera. Using an 8-tap Camera Link configuration allows for transmission of a 2048 x 2048, 8-bit monochromatic image in under 1ms. This high-speed transfer allows for a maximum frame rate of up to 180 frames per second (fps). Using a single aspheric lens with a 405 nm bandpass filter, configured to provide approximately 2.5X magnification, yields a resolution of 0.08 mils per pixel.

The illumination source attached to the camera mount is a 170 mW, 405 nm diode-laser. A laser speckle reducer, model LSR-3005-6D-VIS, with a focusing lens were used with this laser. This

configuration was only used during initial experiments. The radial illumination sources consisted of four 900 mW, 405 nm diode-lasers. With respect to the melt-pool and the camera at 0°, these lasers were positioned at  $\pm 45^\circ$  and  $\pm 135^\circ$  around the melt-pool. No laser speckle reducer or focusing lenses were used for these lasers.

A dedicated PXIe chassis, with a field-programmable gate array (FPGA) and Camera Link adapter module, acquired camera images and system parameters such as laser power, scan speed and position.

The data used in this work was obtained in two sets of experiments. In both sets, scanning speed and laser power undergo step changes from their nominal values, 25 ipm and 350 W respectively, as shown in Figure 2. The first set of experiments utilizes only the 750 mW with laser speckle reduction illumination configuration. While the second set of experiments use only the four radial without laser speckle reduction configuration.

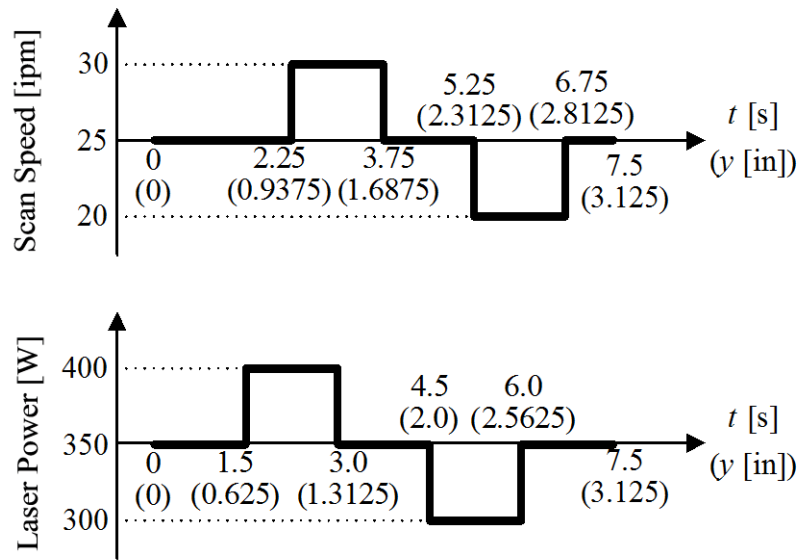


Figure 2. Laser Power and Scan Speed input commands for experiments.

For each experiment data is acquired every 50 ms. Because the camera is mounted to the processing head, the melt-pool remains fixed with respect to the horizontal image plane. This fact allows the image processing algorithm to search along a given vertical vector in order to determine the center of the melt-pool. Once the center of the melt-pool is located, build height and melt-pool width are estimated using threshold detection to determine the boundary between the melt-pool and solidified metal.

The algorithm for determining melt-pool width and build height is tested by manual selection of melt-pool boundaries for each image obtained. Optical profilometry is then used following the experiments to establish a ground truth for melt-pool width and build height. The build height and melt-pool width are determined approximately every 0.0002 in along the deposit, and because scan speed and position are recorded throughout each experiment the optical profilometer data can be

plotted as a function of time or space. This allows for comparison of temporal camera data with spatial profilometer data.

### 3. Results and Data Analysis

Melt-pool width and build height derived from the camera images follow the trends observed in the optical profilometer data. The camera images show a boundary between the melt-pool and solidified metal. However, insufficient illumination results in significant error in the algorithm's estimation of melt-pool geometry. In the first set of experiments the algorithm was unable to find any of the melt-pool boundaries, and manual determination while possible was often extremely difficult as demonstrated by figure 3. Additionally, not all plasma-plume emissions were able to be removed at this level of illumination.

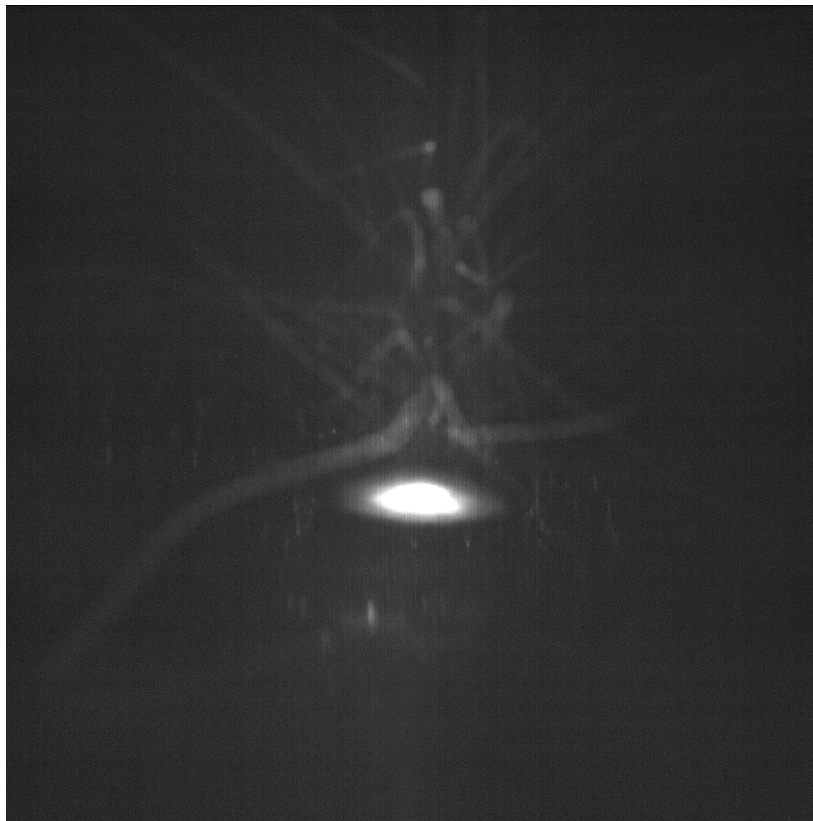


Figure 3. Camera image at time 2.5 seconds during first set of experiments.

In the second set of experiments, the additional illumination provided by the array of radial laser sources allowed the algorithm to determine melt-pool boundaries as demonstrated by figure 4 and figure 5. In addition, unlike the first set of experiments, this level of illumination is sufficient to completely remove interference caused by plasma-plume emissions.

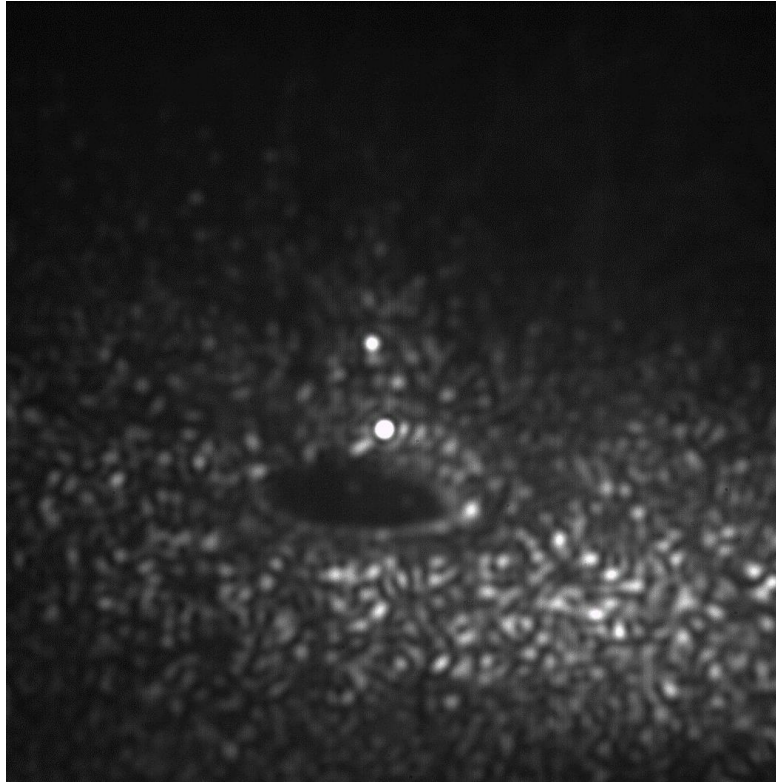


Figure 4. Camera image at time 2.5 seconds during second set of experiments.

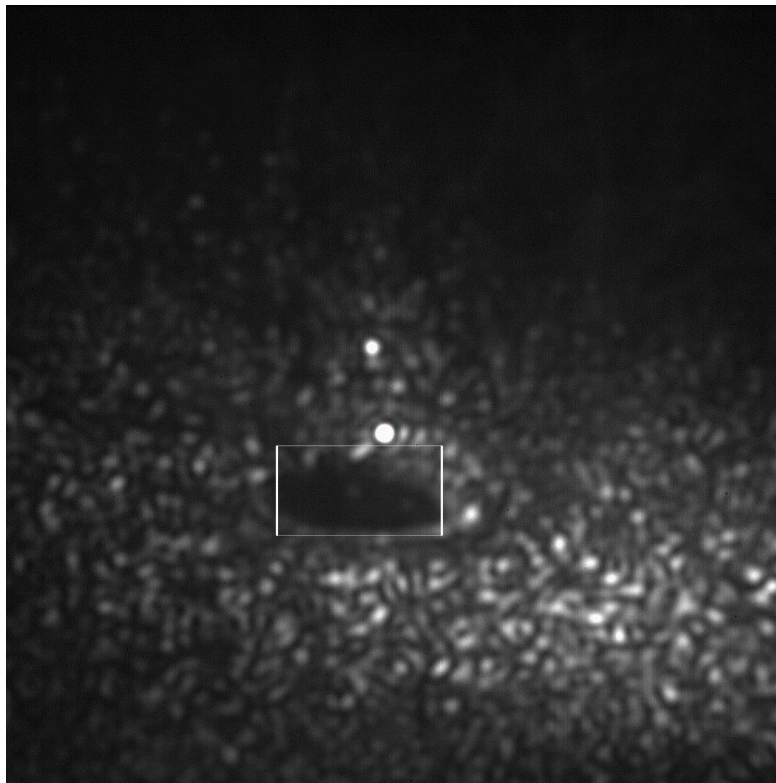


Figure 5. Camera image at time 2.5 seconds during second set of experiments with build height and melt-pool width parameter box drawn as estimated by melt-pool geometry algorithm.

A comparison between the algorithm's boundaries and manually selected boundaries reveals that the illumination was insufficient to provide an acceptable signal-to-noise ratio, resulting in significant error of melt-pool geometry estimates. Figures 6 and 7 show a closer look at relative pixel intensities along the vertical and horizontal search vectors used for estimating build height and melt-pool width respectively. The vertical search vector is a constant vector along the processing laser's position selected through calibration images prior to processing. The horizontal search vector is selected by the algorithm during processing based on the estimated build height and boundary positions on the camera image. Poorly defined boundary points results in estimation error by the boundary algorithm.

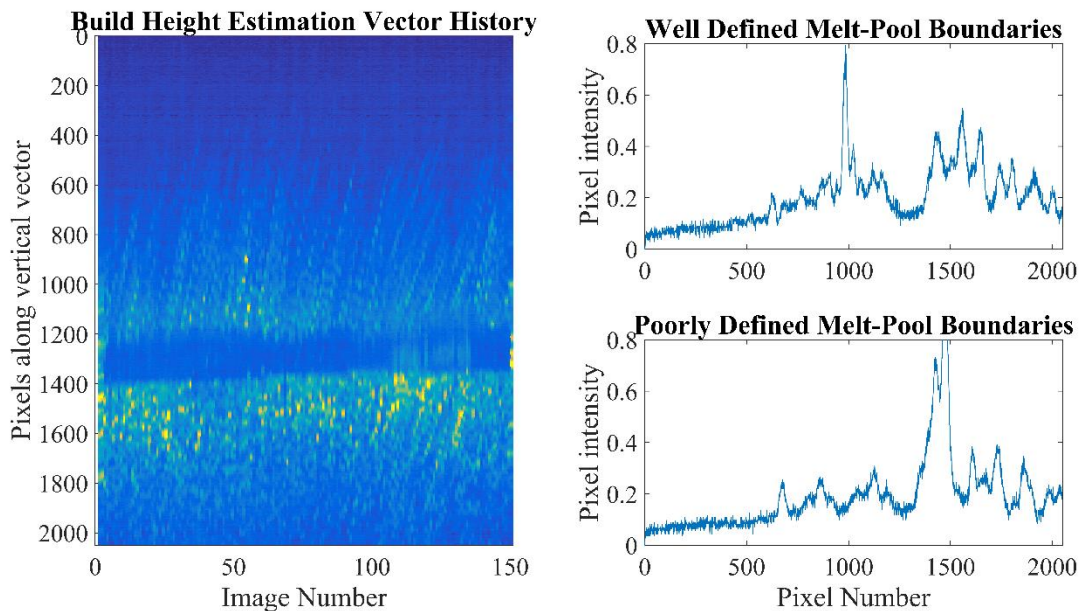


Figure 6. Pixel intensities along build height search vector over time (left). Examples of a well-defined set of height boundaries (top-right) compared to a set of poorly-defined boundaries (bottom-right) for the same scan speed and laser power settings.

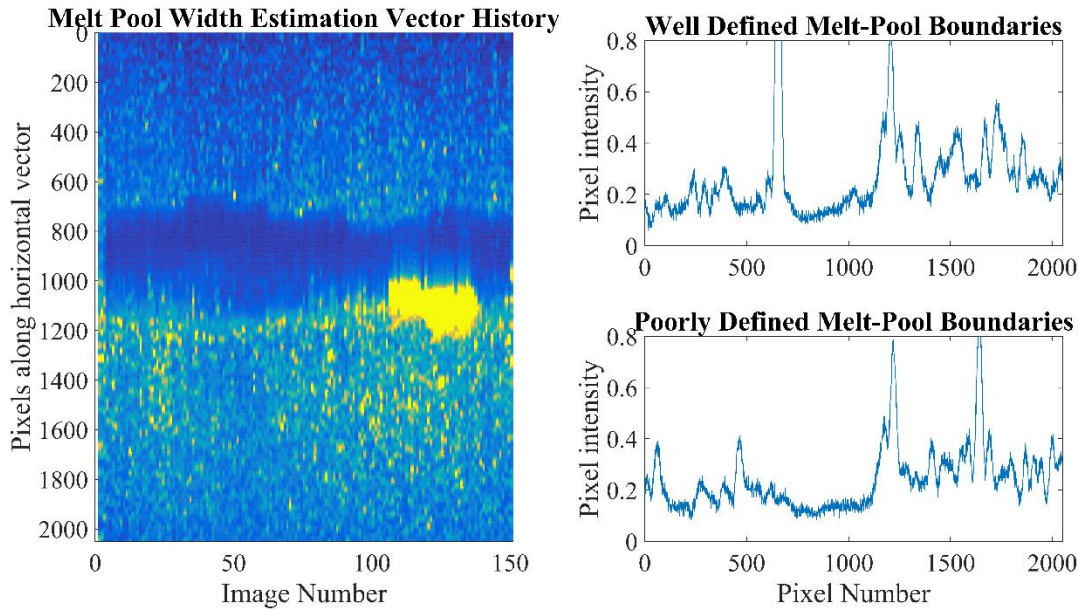


Figure 7. Pixel intensities along width search vector over time (left). Examples of a well-defined set of width boundaries (top-right) compared to a set of poorly-defined boundaries (bottom-right) for the same scan speed and laser power settings.

A comparison of both manual and algorithmic camera estimates to profilometer data shows in figures 8 and 9 that image measurements follow profilometer trends. However, this comparison also reveals that a sample rate of 50 ms is an insufficient sampling rate. The lack of sharp transitions for camera data following a step-change in a system input reveals that these expected output changes are occurring unobserved in between image samples. Because the end goal is to design a control system, it is desirable to have a sample rate such that there are at least 5 samples during a step-transition [2].

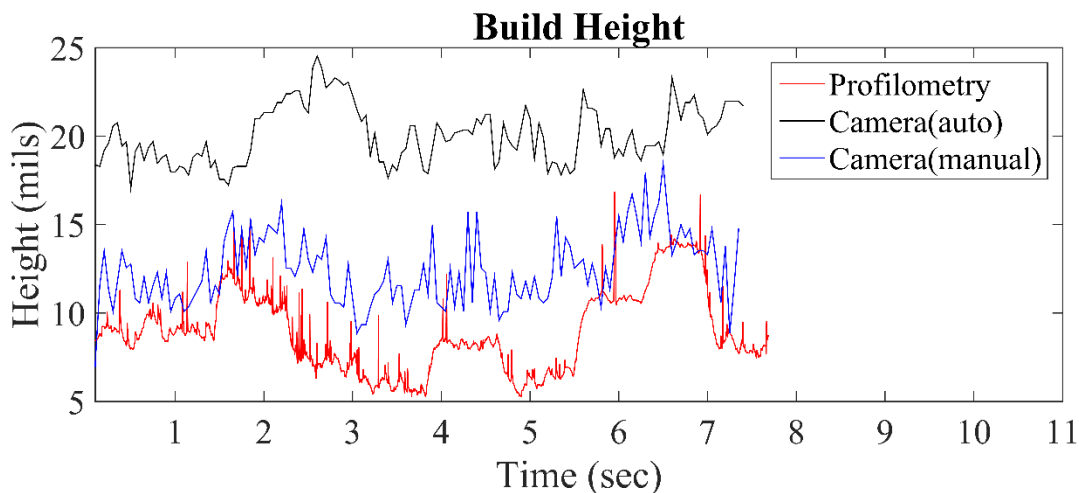


Figure 8. Comparison graph of build height obtained from measurements of manual boundaries, algorithmic boundaries, and optical profilometer data.

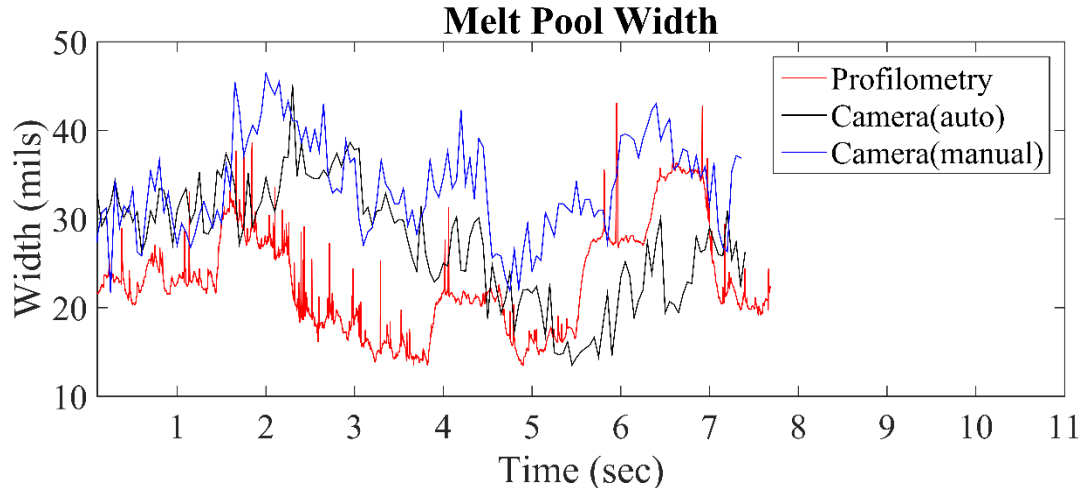


Figure 9. Comparison graph of melt-pool width obtained from measurements of manual boundaries, algorithmic boundaries, and optical profilometer data.

#### 4. Conclusion

The results of this study show that 405 nm is a viable wavelength to observe the AM process without interference from either black body or plasma-plume emissions. Our current configuration will require additional illumination for future experiments. By providing additional illumination, we can ensure that the melt-pool geometry algorithm can accurately and reliably estimate melt-pool boundaries. Additionally, providing more illumination will allow for a reduction in the camera's exposure rate which was the primary limiting factor in determining the sample rate used during these experiments.

Once the illumination system has been improved to provide the necessary amount of illumination for real-time observation of melt-pool geometry, system identification and process models can be created based on real-time images. This will allow for the design of a multi-input multi-output system that can regulate build height and melt-pool width using laser power and scan speed.

#### Acknowledgements

The authors would like to thank Ms. Dalonia O. Lenoir and Dr. Timothy B. Tighe for their assistance with the Optical Profilometry measurements. This work was supported by the Office of Naval Research, under Contract No. N00014-11-1-0668. Any opinions, findings, and conclusions or recommendations expressed in this publication are those of the authors and do not reflect the views of the Office of Naval Research.

#### References

- [1] D. Seltzer, X. Wang, A. Nassar, J. Schaino, and E. Reutzel, "System identification and feedback control for directed-energy metal-based additive manufacturing," in *Solid Freeform Fabrication Proceedings*, Austin, TX. 2015.
- [2] Charles L. Phillips and H. Troy Nagel. *Digital Control Systems Analysis and Design*, third edition, Prentice Hall, 1995.